Inorganica Chimica Acta 363 (2010) 418–423

Contents lists available at ScienceDirect

Inorganica Chimica Acta

journal homepage: www.elsevier.com/locate/ica

Synthesis of the donor–acceptor ligand 2-(4-dimethylaminobenzylidene)-4,5-bis(diphenylphosphino)-4-cyclopenten-1,3-dione (dbpcd) and X-ray diffraction structure of the platinum(II) compound $PtCl_2(dbpcd)\cdot 1.5CH_2Cl_2$

Silvia Atim [a], Xiaoping Wang [b,*], Michael G. Richmond [c,*]

[a] Department of Chemistry and Physics, Coastal Carolina University, Conway, SC 29528, United States
[b] Neutron Scattering Science Division, Oak Ridge National Laboratory, Oak Ridge, TN 37831, United States
[c] Department of Chemistry, University of North Texas, Denton, TX 76203, United States

ARTICLE INFO

Article history:
Received 3 May 2009
Received in revised form 26 October 2009
Accepted 10 November 2009
Available online 14 November 2009

Keywords:
Platinum compounds
Diphosphine ligand
Redox chemistry
MO calculations
Crystallography

ABSTRACT

Knoevenagel condensation of 4-(dimethylamino)benzaldehyde with 4,5-bis(diphenylphosphino)-4-cyclopenten-1,3-dione (bpcd) gives the donor–acceptor ligand 2-(4-dimethylaminobenzylidene)-4,5-bis(diphenylphosphino)-4-cyclopenten-1,3-dione (dbpcd). The reaction of dbpcd with $PtCl_2(cod)$ affords the platinum(II) complex $PtCl_2(dbpcd)$ in high yield. The free dbpcd ligand and $PtCl_2(dbpcd)$ have been isolated and fully characterized in solution by IR and NMR spectroscopies, and the solid-state structure of $PtCl_2(dbpcd)$ determined by X-ray diffraction analysis. $PtCl_2(dbpcd)$, as the $1.5CH_2Cl_2$ solvate, crystallizes in the triclinic space group $P\bar{1}$, $a = 11.7412(7)$ Å, $b = 12.0486(7)$ Å, $c = 14.4781(9)$ Å, $\alpha = 82.866(1)$, $\beta = 75.049(1)$, $\gamma = 83.905(1)$, $V = 1957.6(2)$ Å^3, $Z = 2$, and $D_{calc} = 1.678$ mg/m^3, $R = 0.0291$ and $wR_2 = 0.0723$ for 8315 reflections with $I > 2\sigma(I)$. The molecular structure of $PtCl_2(dbpcd)\cdot 1.5CH_2Cl_2$ consists of a square-planar platinum architecture containing two chlorines and the ancillary dbpcd diphosphine ligand. The redox properties of the dbpcd ligand and $PtCl_2(dbpcd)$ have been explored by cyclic voltammetry, and these data are discussed with respect to extended Hückel MO calculations.

1. Introduction

The synthesis and photophysical study of new inorganic and organometallic compounds that can efficiently promote energy- and electron-transfer reactions remain under are active investigation due to their importance as integral components in artificial photosynthetic mimics, molecular wires, and directional charge-transfer processes [1–4]. The preparation of new luminescent complexes continues to command the attention of researchers in the inorganic and materials communities, with square-planar platinum(II) compounds accounting for the vast majority of published reports [5–7]. The ability to control or manipulate the physiochemical properties of platinum(II) compounds through the tuning of the HOMO and/or LUMO levels is critical if the excited-state properties of a molecule are to be successful exploited for applications involving pH sensors and redox switches.

The redox-active ligand 4,5-bis(diphenylphosphino)-4-cyclopenten-1,3-dione (bpcd) is of interest to our groups because of the low-lying π^* orbital that renders this diphosphine an excellent electron reservoir in chemical and electrochemical reactions involving electron transfer [8–11]. Since the redox properties of the parent ligand and organometallic compounds containing this ligand have been fully described by several different groups, we now have turned our attention toward the functionalization of the dione ring of the parent diphosphine. Our goal of ligand modification is readily accomplished through the Knoevenagel condensation reaction, with the diphosphine ligand serving as the active hydrogen compound given the presence of the 1,3-dione moiety. We have coupled the bpcd ligand with sundry aldehydes to produce the new, second-generation ligands depicted in Scheme 1 [12–14]. Depending on the extent of conjugation between the dione platform and aldehyde appendage, these dyad arrays range from yellow-orange to dark red in color and exhibit rich redox behavior. Here the π^*-based LUMO remains localized on the dione platform in each case and it is the HOMO that is easily tuned via the chosen aldehyde. For example, the ferrocene condensation product, 2-(ferrocenylidene)-4,5-bis(diphenylphosphino)-4-cyclopenten-1,3-dione (fbpcd), reveals an iron-based HOMO and a $0/1^+$ redox couple displaying an $E_{1/2}$ value of 0.63 V. The HOMO–LUMO energy gap may be further tuned and/or altered upon coordination of the redox-active diphosphine ligand to a transition-metal compound, especially if a filled metal orbital supplants the original ligand-based HOMO upon metal coordination.

Herein we report the synthesis of the new diphosphine ligand 2-(4-dimethylaminobenzylidene)-4,5-bis(diphenylphosphino)-4-cyclopenten-1,3-dione (dbpcd) from bpcd and 4-(dimethylamino)benzaldehyde and its use as an ancillary ligand in the

---

* Corresponding authors. Tel.: +1 940 565 3548 (M.G. Richmond).
E-mail addresses: wangx@ornl.gov (X. Wang), cobalt@unt.edu (M.G. Richmond).

0020-1693/$ - see front matter © 2009 Elsevier B.V. All rights reserved.
doi:10.1016/j.ica.2009.11.011

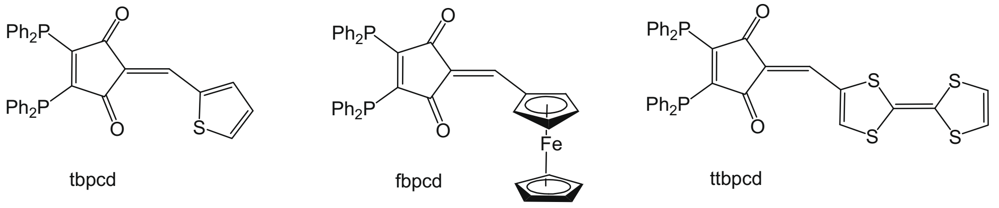

Scheme 1.

platinum(II) compound $PtCl_2$(dbpcd). The solid-state structure of the latter compound has been crystallographically determined, and the redox properties of these new systems have been investigated by cyclic voltammetry. The oxidation and reduction waves recorded by CV are discussed relative to MO calculations performed at the extended Hückel level.

2. Experimental

2.1. Materials and equipment

The $PtCl_2$(cod) was prepared from chloroplatinic acid and 1,5-cyclooctadiene (cod) [15], while the 4,5-bis(diphenylphosphino)-4-cyclopenten-1,3-dione (bpcd) was synthesized from 4,5-dichloro-4-cyclopenten-1,3-dione and Ph_2PSiMe_3 [16,17]. The 4-(dimethylamino)benzaldehyde and potassium *tert*-butoxide were purchased from Aldrich Chemical Co. and used as received. The latter chemical was stored in the dry box when not in use. All reaction solvents were distilled from an appropriate drying agent under inert atmosphere or obtained from an Innovative Technology solvent purification system. All distilled solvents were handled *via* inert-atmosphere techniques, and when not in use these solvents were stored in Schlenk vessels equipped with Teflon stopcocks [18]. The tetra-*n*-butylammonium perchlorate (TBAP) electrolyte was purchased from Johnson Matthey Electronics and recrystallized from a 1:1 mixture of hexane/ethyl acetate and dried under vacuum for at least 44 h prior to use.

The IR spectra were recorded on a Nicolet 6700 FT-IR spectrometer in amalgamated NaCl cells capable of handling air-sensitive samples. The ^{1}H and ^{31}P NMR spectral data were recorded at 500 and 201 MHz, respectively, on a Varian VXR-500 spectrometer. The ^{31}P NMR spectra were collected in the proton-decoupled mode and the reported chemical shifts referenced to external H_3PO_4 (85%), taken to have $\delta = 0$. The ESI-APCI mass spectrum of $PtCl_2$(dbpcd) was recorded at the UNT mass spectrometry facility in the positive ionization mode, using MeOH as the sample matrix.

2.2. Synthesis of 2-(4-dimethylaminobenzylidene)-4,5-bis(diphenylphosphino)-4-cyclopenten-1,3-dione (dbpcd)

To a large Schlenk flask under argon was charged 0.20 g (0.43 mmol) of bpcd, 10 mL of CH_2Cl_2 and 10 mL of MeOH each by syringe, after which 57 mg (0.52 mmol) of $KOBu^t$ was introduced in one portion. 64 mg (0.43 mmol) of 4-(dimethylamino)benzaldehyde was added after 0.5 h and the solution was then gently heated at 40–45 °C for 4 h with stirring. TLC analysis at this point using neutral alumina plates and CH_2Cl_2/hexane (9:1) as the eluent confirmed the consumption of the starting materials and the presence of the desired product at $R_f = 0.67$. The solvents were removed under vacuum and the crude residue purified by column chromatography over neutral alumina using the aforementioned eluent to afford the condensation product dbpcd in 95% yield (0.24 g). IR (CH_2Cl_2): ν(CO) 1713 (w, sym dione), 1662 (vs, antisym dione) cm^{-1}. ^{1}H NMR ($CDCl_3$): δ 2.99 (s, 6H, NMe_2), 6.53 (d, 2H, $^3J_{H-H} = 9$ Hz), 7.15–7.35 (m, 21H, alkenyl and PPh_2 aryl hydrogens), 8.11 (d, 2H, $^3J_{H-H} = 9$ Hz). ^{31}P NMR ($CDCl_3$): δ −23.03 (AB quartet, $^3J_{P-P} = 67$ Hz).

2.3. Synthesis of $PtCl_2$(dbpcd)

To 0.36 g (0.60 mmol) of dbpcd in 20 mL of CH_2Cl_2 was added 0.22 g (0.60 mmol) of $PtCl_2$(cod). The slurry was stirred at room temperature and monitored by TLC using neutral alumina plates until the starting materials were completely consumed (ca. 1 h). The volatiles were next removed under vacuum and the desired product purified by chromatography over neutral alumina using CH_2Cl_2/ethyl acetate (4:1). $PtCl_2$(dbpcd) was obtained as a red-orange solid in 87% yield (0.45 g). Single crystals of $PtCl_2$(dbpcd) suitable for X-ray diffraction analysis were grown at room temperature from a CH_2Cl_2 solution of $PtCl_2$(dbpcd) that had been layered with hexane. IR (CH_2Cl_2): ν(CO) 1726 (w, sym dione), 1668 (s, antisym dione) cm^{-1}. ^{1}H NMR ($CDCl_3$): δ 3.07 (s, 6H, NMe_2), 6.58 (d, 2H, $^3J_{H-H} = 9$ Hz), 7.20–8.16 (m, 23H, alkenyl and aryl). ^{31}P NMR ($CDCl_3$): δ 25.94 (s, $^1J_{Pt-P} = 3660$ Hz), 27.51 (s, $^1J_{Pt-P} = 3660$ Hz). ESI-MS: m/z 826.53 for $[M-Cl]^+$ and 1686.73 for $[2M-Cl]^+$.

2.4. Electrochemical studies

The quoted cyclic voltammetric data were recorded on a PAR Model 273 potentiostat/galvanostat, equipped with positive feedback circuitry to compensate for IR drop. The cyclic voltammograms were recorded under oxygen- and moisture-free conditions in a homemade three-electrode cell. A platinum disk was utilized as the working and auxiliary electrode, and the reference electrode utilized a silver wire as a quasi-reference electrode, with the reported potential data standardized against the formal potential of the $Cp^*_2Fe/Cp^*_2Fe^+$ (internally added) redox couple, taken to have $E_{1/2} = -0.20$ V [19].

2.5. Extended Hückel MO calculations

The extended Hückel calculations on the dbpcd ligand and $PtCl_2$(dbpcd) were carried out using the original program developed by Hoffmann [20,21], as modified by Mealli and Proserpio [22]. The weighted Hij's contained in the program were used in the calculations, and the input *Z*-matrices for the two compounds dbpcd-H_4 and $PtCl_2$(dbpcd-H_4) were constructed by using bond distances and angles from the available X-ray structure. The phenyl groups associated with the phosphorus atoms were replaced with hydrogens and P–H bond distances of 1.41 Å were employed in our calculations [23].

2.6. X-ray crystallographic data

The X-ray data for $PtCl_2(dbpcd)\cdot 1.5CH_2Cl_2$ were collected on an APEX II CCD-based diffractometer at 100(2) K. The frames were integrated with the available APEX2 [24] software package using a narrow-frame algorithm, and the structure was solved and refined using the SHELXTL program package [25]. The phenyl groups on P(2) were found disordered in two positions and refined accordingly with distance restraints. The molecular structure was checked using PLATON [26], and all non-hydrogen atoms were refined anisotropically. All hydrogen atoms were assigned calculated positions and allowed to ride on the attached carbon atom. The refinement for $PtCl_2(dbpcd) \cdot 1.5CH_2Cl_2$ converged at $R = 0.0291$ and $wR_2 = 0.0723$ for 8315 independent reflection with $I > 2\sigma(I)$. The X-ray data and processing parameters are reported in Table 1, with selected bond distances and angles quoted in Table 2.

3. Results and discussion

3.1. Synthesis and spectroscopic properties of 2-(4-dimethylaminobenzylidene)-4,5-bis(diphenylphosphino)-4-cyclopenten-1,3-dione (dbpcd)

The Knoevenagel condensation between bpcd and 4-(dimethylamino)benzaldehyde proceeds smoothly in MeOH solvent with a measured excess of $KOBu^t$ to furnish the new diphosphine ligand reaction 2-(4-dimethylaminobenzylidene)-4,5-bis(diphenylphosphino)-4-cyclopenten-1,3-dione (dbpcd), whose structure is depicted below. The reaction requires $KOBu^t$ because control experiments conducted in the absence of $KOBu^t$ gave only trace amounts of products. The dbpcd ligand is readily isolated by column chromatography over neutral alumina as a red solid in essentially quantitative yield. The choice of chromatographic support is important in this case because the ligand was found to bind irreversibly to silica gel. The vibrationally coupled dione carbonyl groups exhibit ν(CO) bands at 1713 (w,) and 1662 (vs) cm^{-1} and these frequencies are in accord with other derivatives prepared by us [12–14,27]. The ^1H NMR spectrum recorded in $CDCl_3$ confirmed the absence of the signature resonances of the bpcd methylene group and the formyl moiety of the $4\text{-}Me_2NC_6H_4CHO$. The observed singlet at δ 2.99 is readily assigned to NMe_2 group, and the two doublets at δ 6.53 and 8.11, each of which integrates for 2H, represent the pairwise equivalent hydrogens on the pendant benzylidene moiety. The aryl hydrogens associated with the phosphine moieties and the lone alkenyl hydrogen appear as an overlapping multiplet from δ 7.15–7.35. The ^{31}P NMR spectrum reveals a classic AB quartet at δ −23.03 with a $J/\Delta\nu$ value of 0.51 for the inequivalent PPh_2 moieties in agreement with the formulated structure [28].

Table 1
X-ray crystallographic data and processing parameters for $PtCl_2(dbpcd) \cdot 1.5CH_2Cl_2$.

Crystal system	Triclinic
Space group	$P\bar{1}$
a (Å)	11.7412(7)
b (Å)	12.0486(7)
c (Å)	14.4781(9)
α (°)	82.866(1)
β (°)	75.049(1)
γ (°)	83.905(1)
V (Å^3)	1957.6(2)
Molecular formula	$C_{39.5}H_{34}Cl_5NO_2P_2Pt$
Formula weight	988.96
Formula units per cell (Z)	2
D_{calc} (mg/m^3)	1.6788
λ (Mo Kα) (Å)	0.71073
μ (mm^{-1})	4.043
Absorption correction	Semi-empirical from equivalents
F(0 0 0)	974
Crystal size (mm^3)	0.18 × 0.12 × 0.11
Absorption correction factor	0.6739/0.5364
Total reflections	23486
Independent reflections	8315
Data/restraints/parameters	8315/15/508
R_1[a] ($I \geqslant 2\sigma(I)$]	0.0291
wR_2[b]	0.0723
Goodness-of-fit on F^2	1.119
$\Delta\rho_{max}$, $\Delta\rho_{min}$ (e Å^3)	1.924, −2.175

[a] $R_1 = \Sigma||F_o| - |F_c||/\Sigma|F_o|$.
[b] $R_2 = \{\Sigma[w(F^2_o - F^2_c)^2/\Sigma[w(F^2_o)^2]\}^{1/2}$.

Table 2
Selected bond distances (Å) and angles (°) in $PtCl_2(dbpcd) \cdot 1.5CH_2Cl_2$.

Bond distances	
Pt(1)–P(2)	2.217(1)
Pt(1)–Cl(1)	2.341(1)
N(1)–C(10)	1.346(5)
N(1)–C(13)	1.458(6)
C(1)–C(5)	1.530(5)
C(3)–C(4)	1.474(6)
C(4)–C(5)	1.463(6)
P(1)···P(2)	3.126(1)
Pt(1)–P(1)	2.2206(9)
Pt(1)–Cl(2)	2.3565(9)
N(1)–C(14)	1.445(6)
C(1)–C(2)	1.328(6)
C(2)–C(3)	1.510(5)
C(4)–C(6)	1.371(6)
C(6)–C(7)	1.426(6)
Bond angles	
P(2)–Pt(1)–P(1)	89.59(4)
P(1)–Pt(1)–Cl(1)	178.15(4)
P(1)–Pt(1)–Cl(2)	90.02(3)
C(1)–P(1)–Pt(1)	105.4(1)
C(10)–N(1)–C(14)	121.2(4)
C(6)–C(4)–C(5)	133.5(4)
C(4)–C(6)–C(7)	134.6(4)
P(2)–Pt(1)–Cl(1)	88.88(4)
P(2)–Pt(1)–Cl(2)	176.83(4)
Cl(1)–Pt(1)–Cl(2)	91.45(4)
C(2)–P(2)–Pt(1)	105.7(1)
C(10)–N(1)–C(13)	120.7(4)
C(6)–C(4)–C(3)	119.4(4)

dbpcd

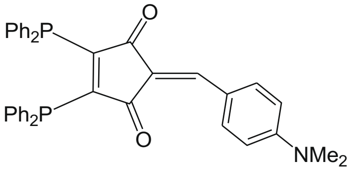

3.2. Synthesis, spectroscopic data, and X-ray diffraction structure of $PtCl_2(dbpcd)$

The dbpcd ligand was next studied for its reactivity with $PtCl_2(cod)$ since the desired compound $PtCl_2(dbpcd)$ can serve as platform for further architectural modification through halide replacement. Treatment of dbpcd with one equivalent of $PtCl_2(cod)$ at room temperature gives the corresponding diphosphine-substituted compound $PtCl_2(dbpcd)$ without complications. $PtCl_2(dbpcd)$ was conveniently isolated by chromatographic separation over neutral alumina, after which the desired product was characterized by a combination of IR and NMR spectroscopies, mass spectrometry, and X-ray diffraction analysis. The IR spectrum for $PtCl_2(dbpcd)$ displays dione ν(CO) bands at 1726 and 1668 cm^{-1} that are shifted slightly to higher energy vis-á-vis the free ligand. The ^1H NMR resonances observed at δ 3.07 and 6.58 are assigned to the NMe_2 group and a pair of aryl hydrogens on the benzylidene ring, respectively. The remaining alkenyl and aryl hydrogens appear as a multiplet from δ 7.20–8.16. The two ^{31}P singlets recorded at δ 25.94 and 27.51 and their accompanying ^{195}Pt satellites of 3660 Hz are consistent with the proposed structure and in keeping with other platinum(II) compounds containing a chelating diphosphine and two chlorine ligands [29]. The ESI mass spectrum of $PtCl_2$(dbpcd) recorded in MeOH gave a weak *m*/*z* peak at 826.53 $[M-Cl]^+$ for the loss of a chloride ion from $PtCl_2$(dbpcd), along with a strong *m*/*z* peak at 1686.73 $[2M-Cl]^+$ arising from the complexation of $[PtCl(dbpcd)]^+$ with $PtCl_2$(dbpcd). The ability of the ESI-MS technique to control aggregation states and guide chemical synthesis as a function of the applied cone angle voltage is a well-established phenomenon [30].

Fig. 1 shows the thermal ellipsoid plot of the molecular structure of $PtCl_2$(dbpcd), as the $1.5CH_2Cl_2$ solvate, and confirms the coordination of the dbpcd ligand to a square-planar platinum(II) center. The Pt–P and Pt–Cl bonds display a mean distance of 2.219 Å and 2.349 Å, respectively, and agree with those distances reported by us for $PtCl_2$(bpcd), $PtCl_2$(fbpcd), and $PtCl_2$(abpcd) [14,27]. The P(1)–Pt(1)–P(2) bond angle of 89.59(4) is typical for this genre of compound and is in excellent agreement with the P–Pt–P angle exhibited by the aforementioned bpcd and bpcd-substituted Pt(II) compounds and the related diphosphine-substituted compounds $PtCl_2$(dppe) and $PtCl_2[(Z)\text{–}Ph_2PCH{=}CHPPh_2]$ [31–33]. $PtCl_2$(dbpcd) exhibits an extended planar array of atoms involving the platinum metal, the platinum-bound chlorine and phosphorus atoms, and the π system defined by the dione and benzylidene fragments. If the four phenyl rings and all of the hydrogen atoms are excluded, the remaining atoms are planar with a $\sigma_p = 0.02$ Å. The bond distances and angles associated with the dione and benzylidene moieties are unremarkable and require no comment.

3.3. Cyclic voltammetric properties and MO calculations on dbpcd and $PtCl_2$(dbpcd)

The redox properties of the dbpcd ligand and $PtCl_2$(dbpcd) were next examined by cyclic voltammetry (CV) in CH_2Cl_2 containing 0.25 M TBAP as the supporting electrolyte. The CV of dbpcd (not shown) recorded over the potential range of 1.0 V to −1.3 V and at a scan rate of 200 mV/s revealed two diffusion-controlled waves at $E_p^a = 0.85$ and −1.14 V, assigned to a multielectron oxidation process and a reversible $0/1^-$ redox couple, respectively [34]. The oxidation wave showed no sign of reversibility up to a scan rate of 1.0 V/s and was not examined further. The site of these redox waves was verified by extended Hückel MO calculations on the model compound dbpcd-H_4, which revealed HOMO and LUMO levels at −11.69 eV and −10.41 eV, respectively. The HOMO is best described as a ligand-based π orbital involving the benzylidene and dione rings, as depicted below. In terms of the fragment contributions to the HOMO, molecular orbital overlap population (MOOP) analysis indicated approximately 80% and 20% contributions from the Me_2N-substituted benzylidene and dione rings, respectively. The orbital composition of the Me_2N-substituted benzylidene ring closely resembles the b_1 HOMO reported for dimethylaniline, a feature consistent with perturbation molecular orbital (PMO) theory [35], with the π system on the dione ring showing a nodal pattern consistent with the Ψ_3 MO exhibited by related 6e-π systems such as hexatriene and maleic anhydride [36]. The π* LUMO found for the new ligand is localized exclusively on the dione moiety with small orbital contributions (<5%) from the PH_2 moieties, as established by MOOP analysis. The energy level and Ψ_4 parentage of the LUMO are features that have already been described in the literature and require no additional comments [10–12].

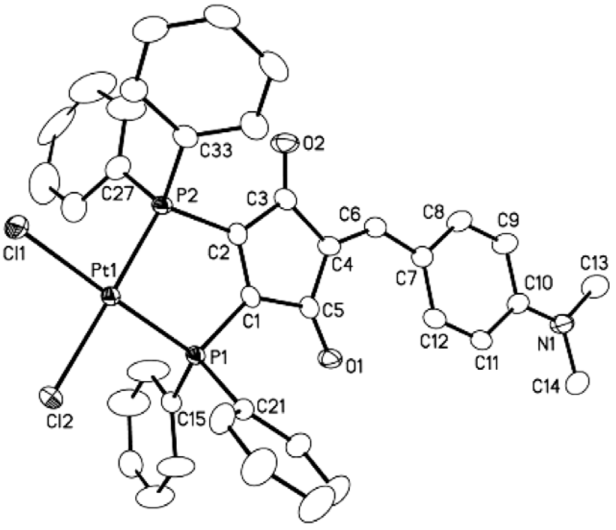

Fig. 1. Thermal ellipsoid plot of $PtCl_2(dbpcd)\cdot1.5CH_2Cl_2$ at the 50% probability level with the hydrogen atoms shown as small spheres of arbitrary radii. The CH_2Cl_2 solvent has omitted for clarity.

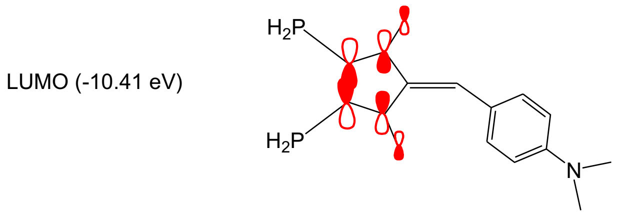

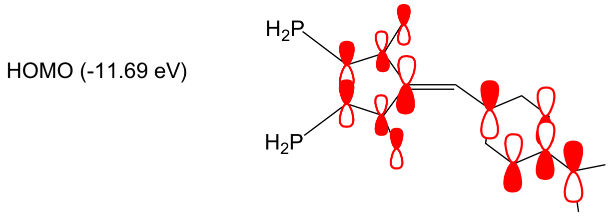

The CV of $PtCl_2$(dbpcd) recorded at 200 mV/s in CH_2Cl_2 containing 0.25 M TBAP as the supporting electrolyte over the potential range of 1.5 V to −1.0 V showed two distinct waves at $E_{1/2} = 1.07$ and −0.65 V that are ascribed to the $0/1^+$ and $0/1^-$ redox couples, respectively. While the oxidation couple in $PtCl_2$(dbpcd) exhibits greater reversibility compared to oxidation wave recorded for dbpcd, it is best viewed as quasi-reversible given the observed current ratio (I_p^c/I_p^a) of 0.80. Increasing the scan rate up to 1.0 V/s led to a slight enhancement in the reversibility of the oxidation based on an I_p^c/I_p^a value of 0.90. The one-electron reduction was judged to be reversible, on the basis of unity current ratios and current calibration against the one-electron standard ferrocene. Extended Hückel calculations were performed to clarify the nature of the HOMO and LUMO in $PtCl_2$(dbpcd). The formal coordination of the $PtCl_2$ fragment to dbpcd does not alter the nature of the HOMO in $PtCl_2$(dbpcd-H_4), as its orbital composition and −11.69 eV energy level are identical to the dbpcd ligand discussed previously. The LUMO level in $PtCl_2$(dbpcd) also mimics the LUMO computed for dbpcd in all respects (i.e., *a* π* dione-based orbital at −10.41 eV). The computational data suggest that a HOMO–LUMO transition would involve a π → π* excitation, and this prediction is supported experimentally by UV–vis spectroscopy where $PtCl_2$(dbpcd) shows a solvent-independent visible band at 484 nm ($\varepsilon = 1480$) that is consistent with such an intraligand (IL) electronic transition [37,38]. In comparison, the compound $PtCl_2$(bpcd) exhibits a near-UV absorbance at ca. 320 nm that has been ascribed to Pt → π*(bpcd) MLCT, on the basis of MO calculations [27]. The absence of a long-wavelength IL transition in $PtCl_2$(bpcd) viz-à-viz $PtCl_2$(dbpcd) underscores the importance of the extended π system in the latter compound and its ability to help tune the HOMO–LUMO transition in this family of compounds.

The HOMO-1 level for $PtCl_2$(dbpcd) at −12.07 eV is of interest because it is primarily a metal-based orbital (d_{z2} with some d_{x2-y2} hybridization) that contains minor antibonding chlorine contributions, as shown below. Conceptually speaking, a low-energy excitation from the HOMO-1 level would be expected to populate the LUMO and give rise to a MLCT band in the near-UV spectrum of $PtCl_2$(dbpcd). The dynamics concerning the HOMO–LUMO transition in the present case are easily manipulated, especially if the Me_2N moiety in the ligand-based HOMO is chemically altered by protonation or quaternization. The loss of the lone-electron pair on the nitrogen atom will lead to a decrease in the energy of the HOMO, as predicted by PMO theory, and promote the HOMO-1 level to that of the new HOMO. In fact, this prediction has been demonstrated by performing MO calculations on the methylated species $[PtCl_2(\text{dbpcd-Me})]^+$, whose nitrogen contribution to the HOMO has been eliminated by methylation. The HOMO in the cationic compound corresponds to the metal-based MO shown below. This is important since the dbpcd-substituted complex may be used as a pH sensor and multipurpose molecular switch through the use of the different IL and MLCT spectral responses.

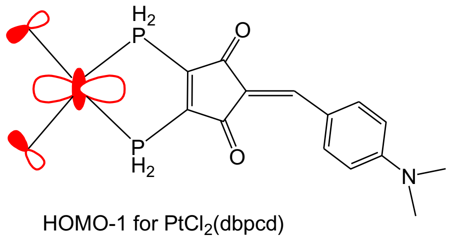

HOMO-1 for $PtCl_2$(dbpcd)

Finally, the behavior of $PtCl_2$(dbpcd) may be contrasted with the redox and MO data exhibited by the parent compound $PtCl_2$(bpcd) compound and the Knoevenagel-modified derivatives containing the ferrocene-substituted ligand fbpcd (*vide supra*) and the ligand 2-(9-anthracenylidene)-4,5-bis(diphenylphosphino)-4-cyclopenten-1,3-dione (abpcd) [27]. Table 3 summarizes the redox and MO data for the related Pt(II) compounds. While the LUMO remains unchanged and is based on a π* MO that is localized on the cyclopenten-1,3-dione platform, it is the HOMO that is easily modulated through the aldehyde that is employed in the Knoevenagel condensation. As mentioned earlier, the HOMO in the fbpcd-substituted compound is similar to the HOMO found in ferrocene, while the π-based HOMO in the abpcd-substituted compound displays b_{2g} symmetry identical to the computed HOMO in anthracene [39]. The functionalization of bpcd with aldehydes more electron rich than 4-(dimethylamino)benzaldehyde or ferrocenecarboxaldehyde is predicted to furnish new diphosphine ligands possessing small HOMO–LUMO gaps, making them ideal candidates as ancillary ligands in Pt(II) compounds for light-harvesting and water-splitting applications.

Table 3
Redox and MO properties of related $PtCl_2$(diphopshine) compounds[a].

Compound	$E_{1/2}(0/1)$	$E_{1/2}$ $(0/1^-)$	HOMO	LUMO	References
$PtCl_2$(bpcd)	–	−0.50	−11.96	−10.36	[27]
$PtCl_2$(fbpcd)	0.62[b]	−0.63	−11.82	−10.35	[14]
$PtCl_2$(abpcd)	–	−0.43	−11.67	−10.40	[27]

[a] The cyclic voltammetry data were recorded in CH_2Cl_2 at room temperature containing 0.20–0.25 M TBAP as the supporting electrolyte over the potential range of 1.0 to −1.0 V at a scan rate of 250 mV/s. The quoted HOMO and LUMO energies are in eV and from extended Hückel calculations.

[b] The observed oxidation wave is localized at the ferrocene portion of the ligand.

4. Conclusions

The new diphosphine ligand 2-(4-dimethylaminobenzylidene)-4,5-bis(diphenylphosphino)-4-cyclopenten-1,3-dione (dbpcd) has been synthesized and used as a ligand in the preparation of the platinum(II) compound $PtCl_2$(dbpcd), whose solid-state structure has been determined by X-ray crystallography. The redox properties of dbpcd and $PtCl_2$(dbpcd) have been explored by electrochemical measurements, and these properties are correlated with the HOMO and LUMO levels established by Hückel MO calculations. The presence of the electron-donating 4-dimethylaminobenzylidene moiety in the dbpcd ligand gives rise to an energetically accessible HOMO in both the free dbpcd ligand and the title Pt(II) compound relative to the parent diphosphine ligand (bpcd) and the $PtCl_2$(bpcd). Future photophysical and luminescence studies are planned, and the use of $PtCl_2$(dbpcd) as a precursor for the synthesis of more highly conjugated, visible-light absorbing systems will be pursued. The details from these studies will be disseminated in due course.

5. Supplementary material

CCDC 728874 contains the supplementary crystallographic data for $PtCl_2(\text{dbpcd})\cdot 1.5CH_2Cl_2$. These data can be obtained free of charge from The Cambridge Crystallographic Data Centre via www.ccdc.cam.ac.uk/data_request/cif.

Acknowledgments

Financial support from the Robert A. Welch Foundation (Grant B-1093-MGR) is greatly appreciated. X. Wang acknowledges the support by the US Department of Energy, Office of Science, under Contract No. DE-AC05-00OR22725 managed by UT Battelle, LLC. Ms. Nicole Ledbetter is thanked for recording the ESI mass spectrum of $PtCl_2$(dbpcd).

References

[1] S. Barlow, D. O'Hare, Chem. Rev. 97 (1997) 637.
[2] V.W.W. Yam, Acc. Chem. Res. 35 (2002) 555.
[3] D. Gust, T.A. Moore, A.L. Moore, Acc. Chem. Res. 34 (2001).
[4] M. Hissler, J.E. McGarrah, W.B. Connick, D.K. Geiger, S.D. Cummings, R. Eisenberg, Coord. Chem. Rev. 208 (2000) 115.
[5] J. Zhang, P. Du, J. Schneider, P. Jarosz, R. Eisenberg, J. Am. Chem. Soc. 129 (2007) 7726.
[6] B. Yin, F. Niemeyer, J.A.G. Williams, J. Jiang, A. Boucekkine, L. Toupet, H.L. Bozec, V. Guerchais, Inorg. Chem. 45 (2006) 8584.
[7] S.-Y. Chang, J. Kavitha, J.-Y. Hung, Y. Chi, Y.-M. Cheng, E.Y. Li, P.-T. Chou, G.-H. Lee, A.J. Carty, Inorg. Chem. 46 (2007) 7064.
[8] H.J. Becher, D. Fenske, M. Heymann, Z. Anorg. Allg. Chem. 475 (1981) 27.
[9] R. Meyer, D.M. Schut, K.J. Keana, D.R. Tyler, Inorg. Chim. Acta 240 (1995) 405.
[10] H. Shen, S.G. Bott, M.G. Richmond, Organometallics 14 (1995) 4625.
[11] N.W. Duffy, R.R. Nelson, M.G. Richmond, A.L. Rieger, P.H. Rieger, B.H. Robinson, D.R. Tyler, J.C. Wang, K. Yang, Inorg. Chem. 37 (1998) 4849.
[12] W.H. Watson, D. Wiedenfeld, A. Pingali, B. Poola, M.G. Richmond, Polyhedron 26 (2007) 3577.
[13] W.H. Watson, B. Poola, M.G. Richmond, Polyhedron 26 (2007) 3585.
[14] B. Poola, S.W. Hunt, X. Wang, M.G. Richmond, Polyhedron 27 (2008) 3693.
[15] D. Drew, J.R. Doyle, Inorg. Synth. 28 (1990) 346.
[16] D.T. Mowry, J. Am. Chem. Soc. 72 (1950) 2535.
[17] D. Fenske, H.J. Becher, Chem. Ber. 108 (1975) 1975.
[18] D.F. Shriver, The Manipulation of Air-Sensitive Compounds, McGraw-Hill, New York, 1969.
[19] M.F. Ryan, D.E. Richardson, D.L. Lichtenberger, N.E. Gruhn, Organometallics 13 (1994) 1190.
[20] R. Hoffmann, W.H. Lipscomb, J. Chem. Phys. 36 (1962) 2179.
[21] R. Hoffmann, J. Chem. Phys. 39 (1963) 1397.
[22] C. Mealli, D.M. Proserpio, J. Chem. Ed. 67 (1990) 399.
[23] R.C. Weast (Ed.), Handbook of Chemistry and Physics, 56th ed., CRC Press, Cleveland, OH, 1975.
[24] APEX2 Version 2.14, Bruker Advanced Analytical X-ray Systems, Inc., Copyright 2007, Madison, WI.
[25] G.M. Sheldrick, Acta Crystallogr., Sect. A 64 (2008) 112.
[26] A.L. Spek, J. Appl. Cryst. 36 (2003) 7.
[27] S.W. Hunt, X. Wang, M.G. Richmond, J. Mol. Struct. 919 (2009) 34.

[28] F.A. Bovey, Nuclear Magnetic Resonance Spectroscopy, Academic Press, New York, 1969.

[29] G. Petőcz, L. Jászlo, W. Weissensteiner, Z. Csók, Z. Berente, L. Kollár, Inorg. Chim. Acta 303 (2000) 300.

[30] K.E. Neo, H.V. Huynh, L.L. Koh, W. Henderson, T.S.A. Hor, J. Organomet. Chem. 693 (2008) 1628.

[31] L.M. Engelhardt, J.M. Patrick, C.L. Raston, P. Twiss, A.H. White, Aust. J. Chem. 37 (1984) 2193.

[32] W. Oberhauser, C. Bachmann, T. Stampfl, R. Haid, C. Langes, A. Rieder, P. Brüggeller, Inorg. Chim. Acta 274 (1998) 143.

[33] B. Bovio, F. Bonati, G. Banditelli, Gazz. Chim. Ital. 115 (1985) 613.

[34] Electrochemical reversibility and electron stoichiometry were determined via the usual methods, see: P.H. Rieger, Electrochemistry, Chapman and Hall, New York, 1994.

[35] T. Kobayashi, S. Nagakura, Bull. Chem. Soc. Jpn. 47 (1972) 2563.

[36] T.A. Albright, J.K. Burdett, M.-H. Whangbo, Orbital Interactions in Chemistry, Wiley-Interscience, New York, 1985.

[37] The formal charge transfer associated with a HOMO–LUMO transition that involves a $\pi \rightarrow \pi^*$ manifold within a coordinated ligand has been termed an intraligand transition. Such processes are differentiated from those charge transfers where an electron from one portion of the molecule (donor) is promoted to a different portion (acceptor) of the molecule upon optical excitation. For reports of intraligand transition in inorganic and organometallic compounds, see: (a) M.S. Wrighton, D.L. Morse, L. Pdungsap, J. Am. Chem. Soc. 97 (1975) 2073;
(b) H. Kunkely, A. Vogler, J. Photochem. Photobiol. A 103 (1997) 227;
(c) H.A. Nieuwenhuis, D.J. Stufkens, R.-A. McNicholl, A.H.R. Al-Obaidi, C.G. Coates, S.E.J. Bell, J.J. McGarvey, J. Westwell, M.W. George, J.J. Turner, J. Am. Chem. Soc. 117 (1995) 5579.

[38] For the effect of solvent on different types of electronic transitions in inorganic/organometallic complexes, see: G.L. Geoffroy, M.S. Wrighton, Organometallic Photochemistry, Academic Press, New York, 1979.

[39] K.E. Wise, R.A. Wheeler, J. Phys. Chem. 108 (1999) 8279.